ELSEVIER

Construction and Building Materials 17 (2003) 165–179

Construction and Building MATERIALS

www.elsevier.com/locate/conbuildmat

# Salt-induced decay in calcareous stone monuments and buildings in a marine environment in SW France

C. Cardell[a], F. Delalieux[a], K. Roumpopoulos[b], A. Moropoulou[b], F. Auger[c], R. Van Grieken[a,*]

[a]*Department of Chemistry, University of Antwerp (U.I.A.), Universiteitsplein 1, B-2610 Antwerp, Belgium*
[b]*Department of Chemical Engineering, Material Science and Technology Sector, National Technical University of Athens, Zografou Campus, Iroon Polytechniou 9, Zografou, 15780 Athens, Greece*
[c]*Lab. de Construction Civile et Maritime-I.U.T. de La Rochelle, 15, rue de Vaux de Foletier, 17026 La Rochelle Cedex 1, France*

Received 5 December 2000; received in revised form 30 July 2002; accepted 28 August 2002

**Abstract**

Salt weathering can be a hazard with significant cultural and economic implications. Salt-induced deterioration of architectural heritage is considered to be accelerated drastically in marine environments. This article investigates the weathering mechanisms and weathering forms in two calcareous stone types used in monuments and buildings on the SW coast of France. The mineralogical, chemical, textural and pore-system characteristics of freshly quarried and decayed stones from quarry, monuments and buildings were determined, and salts loading identified. The stones' resistance against salt weathering was estimated by comparing calculated crystallisation pressures, which are function of the pore size distribution, with the tensile strengths measured by Auger [Alteration des roches sous influence marine; degradation des pierres en oeuvre et simulation acceleree en laboratoir. These Doctorat d'Etat es Siences. Universite de Poitiers, France (1987)]. Results show that Crazannes sparite and La Pallice micrite behave differently with respect to water and salt-spray absorption and local salt precipitation since their pore networks, which control hydric properties, are different. Therefore, diverse weathering patterns due to salt crystallisation pressures were identified in the stones as influenced largely by their pore size distribution: alveolar weathering and granular disintegration in the sparite vs. flaking and micro-fissuring in the micrite. These mechanisms operate in response to salt inputs from a variety of sources—mainly marine aerosols and atmospheric pollution—as corroborated by the so-called enrichment factors (EFs). Wind is believed to trigger alveolar weathering in the heterogeneous sparite. Short-term observations in La Pallice micrite show rapid salt-induced breakdown through 'fatigue' effects. Determining factors involved in stone deterioration is important in the design of proper interventions for protecting historic buildings.


*Keywords:* Marine environment; Salt weathering; Calcareous stones; Architectural heritage; SW France

## 1. Introduction

Salt weathering is a process of rock disintegration that takes place in a variety of environments and affects many kinds of rocks [2]. Salt weathering is a well-known and widespread geomorphic process [3,4], and is one of the principal causes of deterioration of stonework and masonry used in architectural heritage all over the world [5]. Natural and artificial porous media become contaminated with salts in different ways. Salts can originate from incompatible building materials and inappropriate treatments, air pollution, de-icing treatments and soil. Moisture and ground water rising from foundations are other sources to consider. Some materials may even contain salts inherently. Salt deposition in buildings and monuments at coastal sites is mainly by marine aerosol [6,7]. Mechanical action of salt crystallisation processes can exert pressures capable of destroying even the most resistant stone [8,9]. Stone durability depends on its own intrinsic properties (e.g. mineralogy, texture and structure) and on the environ-

*Corresponding author. Tel.: +32-3-820-2362; fax: +32-3-820-2376.
*E-mail address:* vgrieken@uia.ac.be (R. Van Grieken).

0950-0618/03/$ - see front matter © 2003 Elsevier Science Ltd. All rights reserved.
PII: S0950-0618(02)00104-6

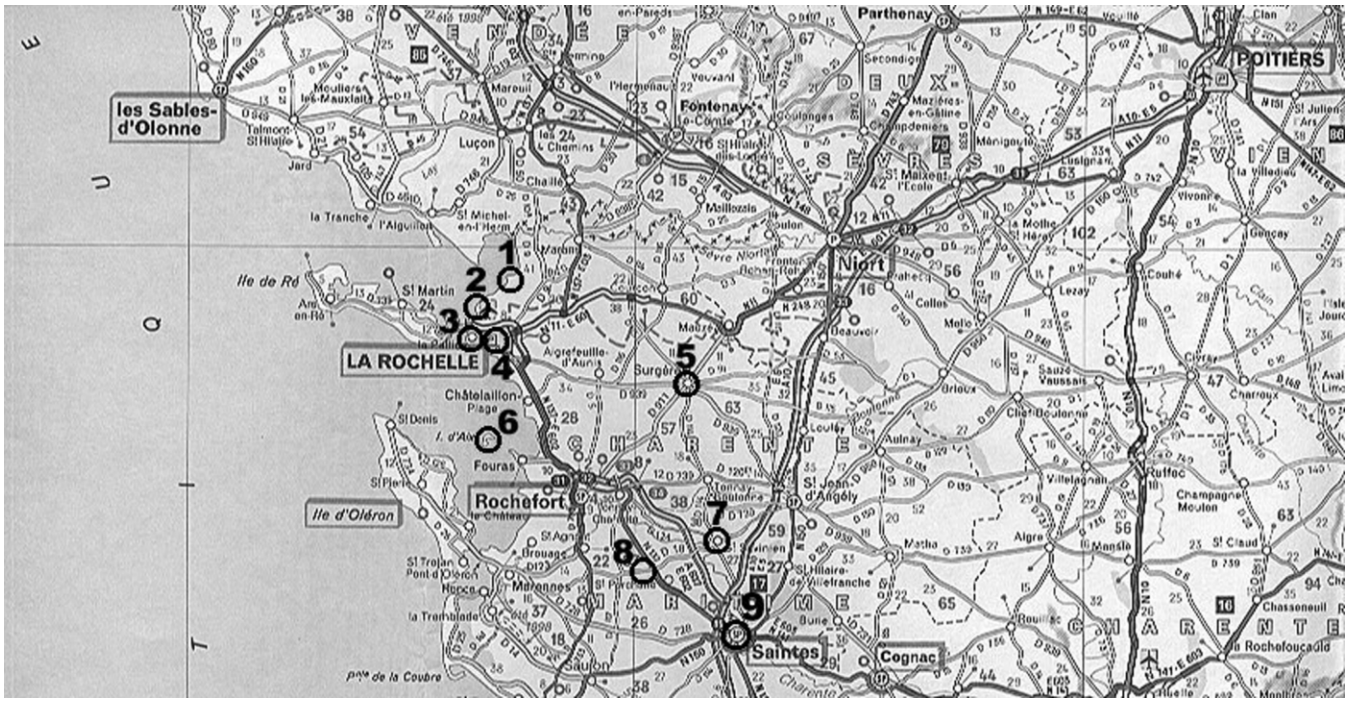


Fig. 1. Selected sampling points in the Aunis province (SW coast of France). 1: Esnandes; 2: Nieul-sur-Mer; 3: La Pallice; 4: La Rochelle; 5: Surgeres; 6: Island of Aix; 7: Saint Savinien; 8: Crazannes; 9: Saintes.

ment to which it is exposed (e.g. air pollution, marine environment, etc.). The combination of these factors leads to different deterioration patterns [10,11].

This article examines salt-induced decay processes which evolved in buildings and monuments in a marine environment on the SW coast of France. The weathering patterns and forms that occur in selected calcareous stones are studied, and their behaviours due to salt crystallisation are predicted from their pore network and tensile strength. In the pursuit of detecting and preventing deterioration of architectural heritage, it is essential to improve the knowledge about the weathering processes that affect the stones used in its construction.

## 2. The study area and sampling campaign

### *2.1. The study area*

The Aunis province is located in the middle Atlantic coast of France, in the Charente-Maritime Department for which La Rochelle is the prefecture. The dryness of this location given its latitude and its maritime character are more typical of a Mediterranean climate. The temperature is moderate with a yearly average of 12.5 °C; the extreme monthly means are 19.3 °C (July) and 5.7 °C (January). Nevertheless, maximum value of 37 °C and minimum of −11 °C have been recorded. The mean annual precipitation is 760 mm, and the average yearly relative humidity is 79%. There are 2250–2500 h of sunshine per year and no more than 25 frost days. The dominant wind directions are NW and SW (from the Atlantic Ocean). Winds favour evaporation from stone surfaces and generation of marine aerosols. According to Auger [1], the marine influence on the alteration of monuments in this region extends as far as 100 km inland.

### *2.2. Monuments and buildings*

Several civil and historical buildings, statues and quarries have been studied in this article (Fig. 1). In La Rochelle, the municipal library, the cemetery of Perigny and the church of Saint Sauvier were sampled. In Saintes, samples were taken from the church of Saint Pierre. Other buildings studied were: the church of Notre Dame in Surgeres; the church of Esnandes; the town hall of the Ile d'Aix; and a memorial statue for the victims of the Second World War in Nieul Sur-Mer. The selected churches found on the pilgrim's route to Santiago de Compostela (Spain) are of Romanesque style: the churches of Surgeres (comprehensively restored in the XIX century); Saint Pierre (XV c.); and Saint Eutrope (XII–XV c.) are all situated 30–40 km from the coast. The other monuments and buildings are located at the coast: the church of Esnandes is enclosed in a massive Gothic fortress; and the church of Saint Sauvier in La Rochelle, besides being exposed to a marine environment, shows substantial evidence of anthropogenic influence. This is the only monument in

which weathering forms due to atmospheric pollution, i.e. black crusts, are in evidence. In the area under study, distinctive degrees of weathering—from moderately to completely weathered stones—can be seen in monuments and buildings.

### 2.3. Stone types

In the Aunis province, quarries are quite numerous and their different calcareous stones (limestones, sandy limestones, marlstones...) largely have been used in the construction of local buildings and monuments. The stones also are exported to different countries (Belgium, England, Germany, Spain…). One of these lithotypes, the St. Savinien stone, was used in the base of the Liberty Statue now in New York. To assess factors involved in salt-induced decay processes in the area, two calcareous stones were selected showing different weathering patterns and forms: Crazannes and La Pallice types, each named after the quarry of origin. In order to establish compositional and textural comparisons between fresh and decayed stones, samples were taken from buildings, monuments and quarries.

Crazannes stone is a macroporous, medium-grained, buff-coloured limestone or sparite [12] of Upper Turonian age (Cretaceous). This stone type has a heterogeneous texture and shows severe alveolar weathering, granular disintegration, efflorescences and subfloresc-ences in buildings, monuments and quarry (Fig. 2a). Black crusts are also observed in monuments. La Pallice stone is a microporous, fine-grained, grey-buff-coloured limestone or micrite [12] with low clay content. It is a compact stone with a homogeneous texture of Lower Kimmeridgian age (Jurassic). This type shows flaking and fissuring (Fig. 2b).

## 3. Experimental procedures

The sampling campaign was carried out according to the following criteria: (I) distance from the coast; (II) type of calcareous stone; (III) weathering forms; and (IV) orientation and height of samples in buildings and monuments (Table 1). Samples were taken more than 2 m above ground level to avoid the influence of moisture from the foundation.

### 3.1. Analytical techniques and methods

Twenty-one samples were studied to characterise freshly quarried and decayed stones from monuments, buildings and quarries. The stone samples were crushed to a fine powder in an agata mortar. Mineralogy of stones and efflorescences was determined with X-ray diffraction (Philips PW1840 diffractometer). Bulk composition of the stones was analysed with energy dispersive X-ray fluorescence (EDX-RF) using a Tracor

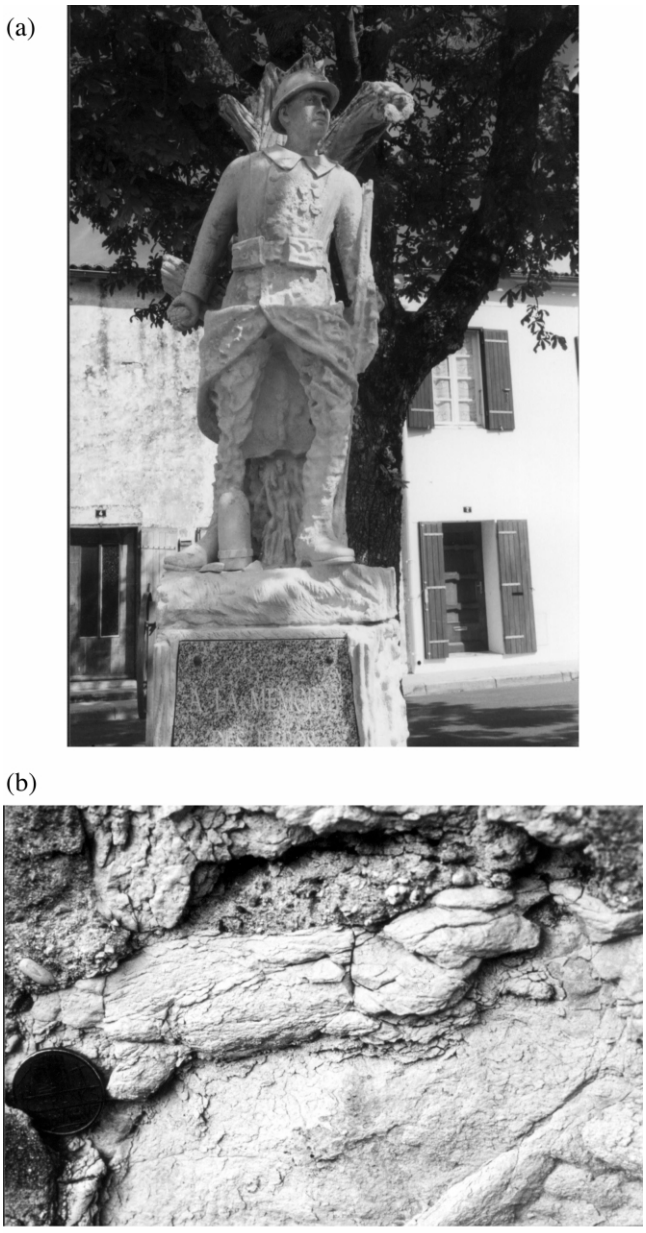

Fig. 2. (a) Alveolar weathering and granular disintegration in a sculpture built with the Crazannes sparite (Nieul Sur-Mer, SW France). (b) Detail of fissuring in the La Pallice micrite (Cemetery of Perigny, La Rochelle).

Spectrace 5000 equipped with a Si(Li) detector. For this end, the powder was wet-ground during 1 min in a McCrone Micronizing Mill, to further reduce the grain size. Approximately 3 ml of the resulting suspension was brought onto a Mylar foil which was glued to a Teflon ring. A homogeneous layer (approx. 1 mg $cm^{-2}$) of sample was obtained after drying the foil at 50 °C in an oven. All spectra were analysed using the AXIL software.

Bulk composition of the leachable fraction (soluble salt content) from the stones was also determined.

Table 1
Description of the studied calcareous stones on the SW coast of France

| Sample | Location | Weathering forms |
|---|---|---|
| CR-1 | Quarry at 30 km from the coast | Fresh sample |
| CR-2 | Quarry at 30 km from the coast | Granular desaggregation, efflorescences |
| CR-2P | Quarry at 30 km from the coast | Efflorescences |
| CR-3 | Quarry at 30 km from the coast | Efflorescences |
| CR-4 | Quarry at 30 km from the coast | Fresh sample |
| CR-M1 | Base of a statue in Nieul Sur-Mer, at the coast. Height = 1.5 m; exposed to overall wind influence | Severe alveolar weathering |
| CR-M2 | Main door of the church of Esnandes, at the coast. Height = 1.5 m; W orientation | Severe alveolar weathering |
| CR-M3 | Main façade of the town hall of Ile d′Aix, at the coast. Height = 1.5 m; S orientation | Severe alveolar weathering, Granular desaggregation, efflorescences |
| CR-M5 | Main door of the church of St Sauvier in La Rochelle, at the coast. H = 1.5 m; W orientation | Severe alveolar weathering |
| CR-M6 | Main door of the church of St Sauvier in La Rochelle, at the coast. Height = 2 m; W orientation | Black crust |
| CR-M7 | Main door of the Municipal Library in La Rochelle, at the coast. Height = 2 m; W orientation | Alveolar weathering |
| CR-M8 | NW façade of the church of Saint Pierre in Saintes, at 40 km from the coast | Alveolar weathering |
| LP-1 | Quarry at the coast; direct exposure to salt bearing wind and spray | Apparently fresh |
| LP-2 | Port, in the splash zone | Multiple flaking |
| LP-M1 | Church of Surgeres, at 30 km from the coast | Flaking, micro-fissuring |
| LP-M5 | Church of Surgeres, at 30 km from the coast | Multiple flaking |
| LP-M2 | Church of Esnandes, at the coast | Flaking, micro-fissuring |
| LP-M3 | Church of Esnandes, at the coast | Flaking |
| LP-M4 | Church of Esnandes, at the coast | Micro-fissuring |
| LP-M6 | A civil building in La Rochelle, at the coast | Flaking |
| LP-M7 | Cemetery of Perigny in La Rochelle, at the coast | Flaking, micro-fissurings |

Weathering forms after Fitzner et al. [10].

Approximately 100 mg of powder sample was dispersed in 100 ml of de-ionised water and placed in an ultrasonic bath for 25 min. The aqueous suspension was filtered through a Millipore filter (pore size 0.2 μm). Anions ($Cl^-$, $NO_3^-$ and $SO_4^{2-}$) were analysed with ion chromatography (IC) using a Dionex 4000I. Cations ($Ca^{2+}$, $Mg^{2+}$, $Na^+$ and $K^+$) were analysed with inductively coupled plasma-atomic emission spectroscopy (ICP-AES) using a Jobin Yvon 124.

Petrographic characteristics of fresh and decayed stones, of which morphology and pore size distribution are important in deterioration mechanisms, were determined via mercury intrusion porosimetry (MIP) using a Pascal 440 unit and a Fisons Porosimeter 2000, and with optical microscopy (Carl Zeiss model Jenapol U). In this article the 0.1-μm pore size is considered as the limit between microporosity and mesoporosity, according to the forces inducing fluid movement through porous media. Thin sections were prepared for study with optical microscopy. Sections perpendicular to the surface of the stone samples were examined with scanning electron microscopy-energy dispersive X-ray analysis (SEM-EDX) using a JEOL-JSM 6300. Distribution, habits and composition of salts with depth into the stones were also studied with SEM-EDX. Data concerning quantification of salts with depth in these stones can be found in Cardell et al. [13]

### 3.2. Seawater contribution to the salts

The seawater contribution to the salts in the stones was estimated. The most usual method for evaluating this contribution is to compare ionic concentration ratios of measured ions to $Na^+$ with those found in seawater [14]. The so-called enrichment factors (EFs) are obtained using the following equation:

$$EF_{\text{soluble salt}}(X) = (X/\text{Na})_{\text{soluble salt}}/(X/\text{Na})_{\text{seawater}}$$

where $X$ denotes the concentration of the measured ion or element, and $Na^+$ denotes the concentration of the indicator element. The average composition of seawater was taken from Ridley and Chester [15]. An EF near unity suggests that seawater is the primary source of the element $X$. Values much higher than unity imply the importance of sources other than seawater for salts. These sources mostly include various anthropogenic activities. In this case elements are termed enriched [16].

### 3.3. Crystallisation pressure

In this article, the pore system characteristics of the stones under study were used to evaluate their potential susceptibilities to salt decay by calculating NaCl crystallisation pressures, since NaCl is the most widespread and abundant salt in the stones [13]. Salt weathering has been reported to be due to the build-up of crystallisation pressure against pore walls when salt nucleation and growth take place in a confined space [17]. Based on the analogy with the theoretical freezing model in porous media developed by Everest [18], first Wellman and Wilson [19] and later Fitzner and Snethlage [20] developed a thermodynamic model for calculating the crystallisation pressure of a salt in a pore. According to Wellman and Wilson [19] salt crystals grow preferentially in the largest pores and the salt solution is withdrawn from the smaller pores. When a crystal fills a large pore, crystallisation can take place in smaller pores connected to it, but the crystal will continue growing and it will generate a pressure $P$ against the pore walls. The excess pressure $\Delta P$, as calculated by Wellman and Willson [21], is correlated with the pore dimensions by Eq. (1):

$$\Delta P = 2\sigma\ (1/r - 1/R) \quad (1)$$

where $\sigma$ is the interfacial tension between the solution and the growing crystal; $r$ is the radius of small pores and $R$ is the radius of coarse pores. The calculated pressure $\Delta P$ is the excess crystallisation pressure built up when crystallisation proceeds from a large pore to a smaller, interconnected one. Thus, when $\Delta P$ exceeds the tensile strength of the stone, fracture of the material will take place. This suggests that in a smaller sized pore the pressure developed by crystal growth is higher than in larger pores. Rossi-Manaresi and Tucci [22] employed this equation to calculate the resistance of different stones to salt deterioration, e.g. biocalcarenites, tuffs, marbles and sandstones.

Recently, a thermodynamic model of crystallisation pressure has been established based on Young-Laplace and Pitzer's models, integrating the effects of supersaturation and size distribution in porous media, which former models use separately [23]. However, lacking data on (time-varying) supersaturation in the stones, we have estimated Na crystallisation pressures that can develop in the studied stones following the method employed by Rossi-Manaresi and Tucci [22]. For this end, pores were grouped according to radii (expressed in millimetre) into five classes in the following ranges: class I, $r<0.01$; class II, $r=0.01-0.1$; class III, $r=0.1-1$; class IV, $r=1-10$; and class V, $r=10-100$. The median radii of pore classes I to IV are: 0.005, 0.05, 0.5, 5 and 50, respectively. Class V ($R=50$ μm) is considered the one where preferential crystal growth takes place. Its radius $R$ is much greater than all the other median $r$-values, therefore $1/R$ can be eliminated in Eq. (1). A more simple equation Eq. (2) can be used without introducing significant error:

$$\Delta P = 2\sigma\ (1/r) \quad (2)$$

The value $\sigma=8.35$ Pa was taken as a reasonable value for NaCl interfacial tension as measured by Rodríguez-Navarro and Dohene [24].

To calculate the effective pressure which can arise in the stones, it is necessary to consider the volume percent of the pores of each class $V_r$ which should be related to the volume percent of coarse pores $V_R$. Multiplying the factor $V_r/V_R$ for the theoretical pressure of each class permits calculation of the effective pressure value $P_e$. The total pressure (tension) the stones will support when NaCl crystallises is the sum of the effective pressure of each pore class.

The disruptive effect of salt crystallisation in porous media is due to the generation of crystallisation pressures which are greater that the cohesive forces of the material. Mechanical resistance of stone is based on tensile strength. In engineering materials, the tensile strength is the quantity which, on a macroscopic level, reflects the cohesive strength of the solid, and governs the maximum load per surface area which can be supported without fracture. When the crystallisation pressure exceeds the tensile strength, the material breaks. Tensile strengths have been deduced from the measured values of simple compression in dry conditions determined by Auger [1], following Griffith's theory [25]. This theory postulates that the strength of brittle materials like rock in compression should be approximately 10 times the tensile strength. With this in mind, the tensile strengths of the studied rocks are as follows: 0.9 MPa for Crazannes sparite; and 6.1 MPa for La Pallice micrite.

## 4. Results

### 4.1. X-Ray diffraction (XRD)

Fresh and decayed stones have similar composition in quarry, monuments and buildings with slight differences (Table 2). Calcite is the major mineral in both Crazannes and La Pallice stones (>90%). In Crazannes sparite quartz is present in trace amounts, gypsum appears in crusts (CR-M6), in efflorescences (CR-2P), and in samples showing alveolar weathering (CR-M5). In La Pallice micrite, quartz is more abundant (15–30%). In quarry stone, decayed samples contain gypsum, halite and phyllosilicates (LP-2). Curiously, halite is not detected in monuments and gypsum is only found in samples affected by flaking.

### 4.2. Energy dispersive X-Ray fluorescence (EDXRF)

The EDX-RF results (Table 3) show that fresh and decayed La Pallice samples contain more Si, K, Ti, Mn,

Table 2
Mineralogy of samples from quarry* and monuments and buildings on the SW coast of France

| Samples | Weathering | Calcite | Quartz | Gypsum | Phyllosilicates | Halite |
|---|---|---|---|---|---|---|
| LP-1* | F | X | | | | |
| LP-2* | D | X | x | | * | |
| CR-1* | F | X | x | | | |
| CR-2P* | D | X | * | * | | * |
| LP-M1 | D | X | x | | | |
| LP-M5 | D | X | x | | | |
| LP-M2 | D | X | x | | | |
| LP-M3 | D | X | x | * | | |
| LP-M4 | D | X | x | | | |
| CR-M1 | D | X | * | | | |
| CR-M2 | D | X | * | | | |
| CR-M3 | D | X | | | | |
| CR-M5 | D | X | * | * | | |
| CR-M6 | D | X | | X | | |

F = fresh samples; D = decayed samples; X = > 90%; x = 15–30%; *trace amounts.

Ni, Rb and Sr than Crazannes samples. The higher concentration of these elements is due to presence of phyllosilicates and Fe-oxi-hydroxides that make up the La Pallice micrite. Decayed La Pallice samples contain larger K amounts than fresh samples (except LP-M5). In Crazannes samples, Fe amounts are lower than in La Pallice samples, except for CR-M1 and CR-M6. Decayed Crazannes samples have more Fe, Cu, Zn and Sr than do fresh ones. Lead (Pb) is only detected in samples from monuments in both La Pallice and Crazannes stones, but mainly in the latter.

### 4.3. Optical microscopy

Fresh and decayed samples have similar texture and mineralogy for each stone type. Crazannes sparite is largely made up of sparry calcite cement (grain size > 10 μm). Fossils, i.e. bryozoans, algae and echinoids are scarce. Small amounts of micas and Fe-oxi-hydroxides (that cannot be detected with XRD) are also identified. Crazannes sparite exhibits two kinds of porosity: intergranular porosity built up of larger pores and intragranular porosity, which is located within the fossils (moldic pores). In decayed samples, pores larger than approximately 0.8 mm were observed, indicating that carbonate cement dissolution is active (Fig. 3a). Porosity diminishes locally near the surface due to salt in-filling pores. Black crusts are made up of carbonaceous particles, quartz and halite embedded in layers of gypsum and clay minerals (Fig. 3b). Halite also is identified below the crust. Granular disaggregation and salt crystallisation were observed at a depth of approximately 1 cm below the surface [13].

La Pallice micrite is a homogenous limestone made up of micritic calcite (grain size <4 μm). A few nodules of calcite (approx. 20 μm) and low proportions of quartz and Fe-oxi-hydroxides are identified. Its pore network comprises few isolated rounded pores smaller than 10 μm (Fig. 4a). Decayed samples show a fissure network parallel to the surface and confined to the first 5 mm from the surface. When few micro-fissures appear in the outermost part of the stone, scales are created parallel to the exposed surface (Fig. 4b). Multiple flaking develops when fissures are more abundant and continue deeper within the stone.

### 4.4. SEM-EDX

Decayed Crazannes samples show etching features in some calcite and quartz grains indicating micro-dissolution processes (chemical weathering). Carbonate cement dissolution and subsequent calcite re-crystallisation are also observed. These processes are more intense in samples from monuments and buildings. Anhedral and subhedral halite crystals and halite layers are found down to a depth of 1 cm into the stones. In contrast, halite is found down to 2 mm beneath the surface in decayed Crazannes samples from quarry.

In decayed La Pallice samples, amorphous layers composed of Si, Al, Mg and Ca, plus S, Cl and Na are identified near the surface (Fig. 5). These elements are considered to form clay minerals, halite and gypsum, since they were detected with XRD. Despite the presence of clay minerals, shrink–swell processes are not observed. Subhedral, cubic and acicular crystals made up of Cl, Ca, or K are identified. In fractures S, Cl and Fe are detected.

### 4.5. Soluble salts

Decayed stones from quarries, monuments and buildings contain more soluble salts than fresh stones (Table 4). The results are shown in milliequivalent per gram in order to provide a measure of the relationship between cations and anions. Decayed Crazannes samples have higher salt contents than decayed La Pallice samples,

Table 3
Bulk composition (EDX-RF) of Crazannes sparite (CR) and La Pallice micrite (LP) on the SW coast of France

| | Al (%) | Si (%) | S (ppm) | K (ppm) | Ca (%) | Ti (ppm) | Mn (ppm) | Fe (ppm) | Ni (ppm) | Cu (ppm) | Zn (ppm) | Rb (ppm) | Sr (ppm) | Pb (ppm) |
|---|---|---|---|---|---|---|---|---|---|---|---|---|---|---|
| LP-1[a,b] | 2.4 | 2.8 | 1100 | 1638 | 38.4 | 408 | 79.3 | 3683 | 6.5 | 5.3 | 22.7 | 16.5 | 366.9 | — |
| LP-2[a] | 1.6 | 3.5 | 1300 | 2420 | 37.9 | 614 | 107 | 3983 | 5.2 | 4.2 | 21.9 | 16.9 | 370.9 | — |
| CR-1[a,b] | 1.6 | 1.1 | — | 988.5 | 40.1 | 85.7 | 24.1 | 304.9 | — | 3.7 | 19.4 | 11.5 | 152.1 | — |
| CR-2P[a] | 2.2 | 1.1 | — | — | 40.7 | 104 | 12.6 | 328.8 | — | 2.2 | 14.7 | 6.10 | 175.7 | — |
| CR-3 | 1.4 | 0.8 | — | 566.8 | 39.6 | 87.2 | 21.8 | 280.3 | — | 4.1 | 24.1 | 6.57 | 184.2 | — |
| CR-4 | 1.8 | 0.75 | 1200 | — | 41.6 | 52.0 | 17.1 | 237.9 | — | 2.9 | 17.2 | 8.47 | 180.5 | — |
| LP-M1 | 1.8 | 2.8 | 1300 | 2188 | 38.1 | 390 | 58.7 | 3014 | 6.0 | 7.5 | 32.7 | 19.1 | 301.1 | — |
| LP-M5 | 2.2 | 2.1 | 930 | 834.7 | 38.8 | 282 | 77.8 | 2779 | — | 3.9 | 21.3 | 18.1 | 282.4 | 47.2 |
| LP-M2 | 3.2 | 4.0 | 1100 | 2892 | 27.1 | 664 | 126 | 4845 | 5.5 | 6.0 | 48.1 | 24.3 | 444.5 | — |
| LP-M3 | 2.9 | 6.1 | 1200 | 3942 | 32.7 | 907 | 189 | 6918 | 8.8 | 7.8 | 38.1 | 30.3 | 473.5 | 35.4 |
| LP-M4 | 2.2 | 5.2 | 750 | 2770 | 28.8 | 968 | 163 | 6566 | 9.8 | 9.6 | 34.4 | 27.8 | 443.1 | — |
| CR-M1 | 2.2 | 1.9 | 1000 | 1090 | 40.3 | 260 | 56.2 | 1914 | — | 5.7 | 29.7 | 12.2 | 217.3 | — |
| CR-M2 | 1.9 | 1.1 | 1100 | 550 | 41.9 | 99.6 | 26.8 | 487.1 | — | 3.3 | 21.7 | 7.60 | 215.3 | — |
| CR-M3 | 2.4 | 1.3 | — | 600 | 41.8 | 133 | 52.1 | 609.1 | — | 11 | 158 | 10.4 | 169.2 | 71.3 |
| CR-M5 | 1.3 | 1.5 | — | 1489 | 38.7 | 117 | 39.1 | 586.7 | — | 22 | 41.9 | 14.6 | 200.1 | — |
| CR-M6 | 1.5 | 1.2 | — | 840.3 | 39.7 | 152 | 64.6 | 1621 | — | 16 | 64.1 | 7.80 | 228.7 | 66.7 |

— = Not detected.
[a] Quarried samples.
[b] Fresh samples.

specifically $SO_4^{2-}$ and $Cl^-$; instead, $NO_3^-$ is more abundant in La Pallice samples. Fresh Crazannes samples contain an identifiable quantity of $Cl^-$ (CR-1 and CR-4), unlike La Pallice samples. The lowest $Cl^-$ contents are found in fresh La Pallice samples from quarry. Nitrate ($NO_3^-$) is more abundant in monument samples than was expected considering that samples originate from either walls affected by biological activity or sites with abundant bird droppings. The highest amounts of $Na^+$ when compared with $Cl^-$ suggest the presence of Na-salts other than halite. This is the case for decayed Crazannes samples in quarry. On the other hand, $Cl^-$ amounts in samples from monuments and buildings are larger than $Na^+$ amounts.

### 4.6. Enrichment factors (EFs)

The results of EFs of soluble salts contained in stones relative to seawater are presented in Table 5. EFs of approximately 1 for $Cl^-$ indicate the marine origin of this element in all samples. Some $SO_4^{2-}$ originates from the sea but anthropogenic sources also are present. Thus, the EFs of 36 and 40 for sample CR-M5 and CR-M6, respectively, suggest atmospheric pollution as a possible

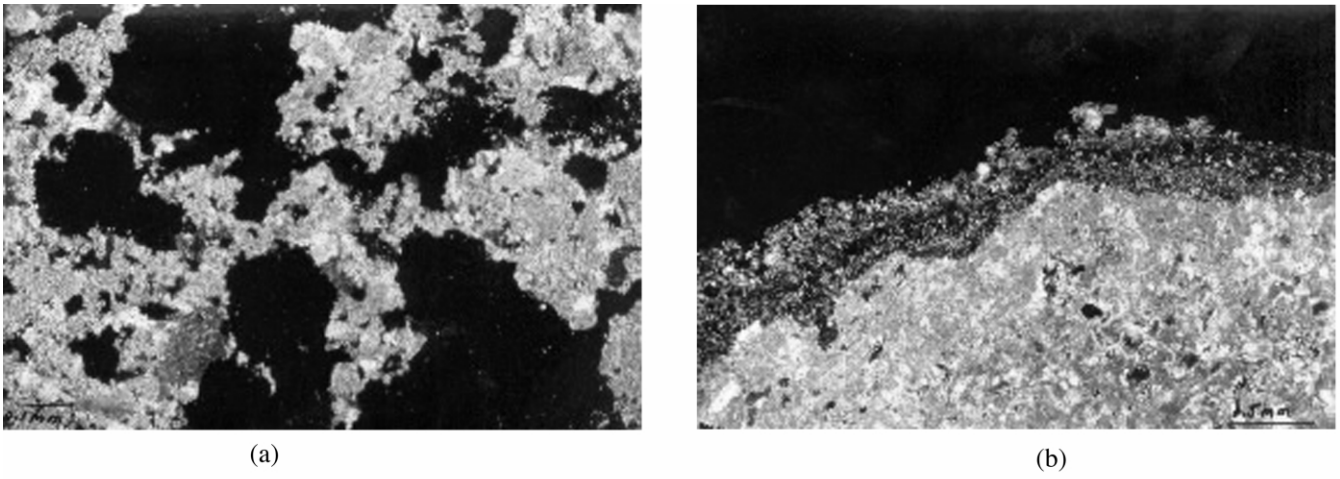

(a) (b)

Fig. 3. Thin-section micrographs of Crazannes sparite (crossed polars). (a) Detail of large pores interconnected due to dissolution of calcitic matrix. (b) Black crust in the stone surface consisting in layers of gypsum, clay minerals, carbonaceous particles and quartz. Halite is also present.

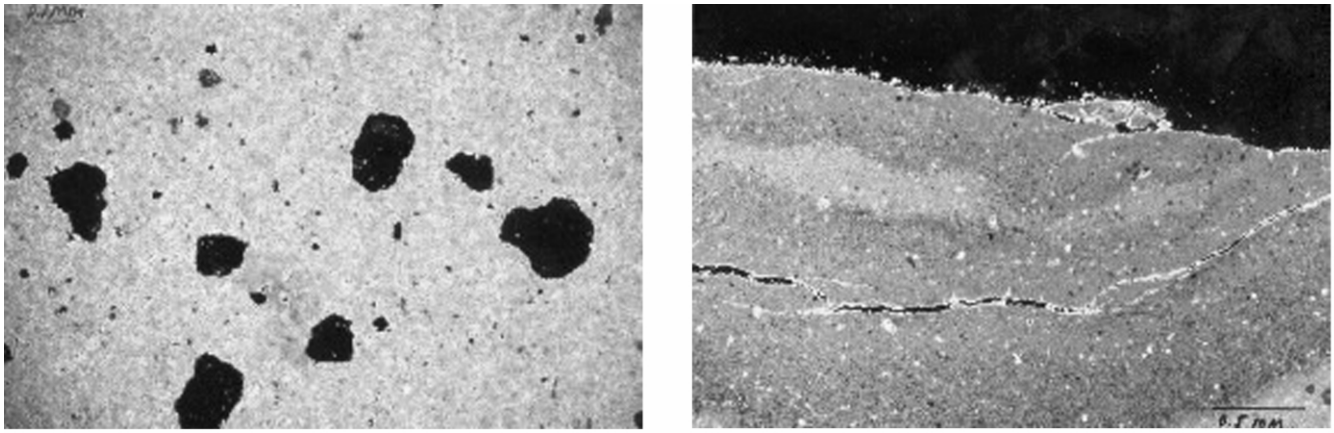


Fig. 4. Thin-section micrographs of La Pallice micrite (crossed polars). (a) Detail of the small and isolated pores. (b) View of the microfissures network developed in the stone surface.

source. Magnesium ($Mg^{2+}$) has a marine origin in all the Crazannes samples. The high EFs for $Mg^{2+}$ in the La Pallice samples suggest sources other than seawater.

### 4.7. Pore structure

The pore system characteristics, i.e. total porosity and pore size distribution, of fresh and decayed samples from quarries, monuments and buildings are shown in Table 6. Freshly quarried samples of both calcareous stone types have similar connected porosity or total porosity (TP): 14.7% for Crazannes sparite and 15.2% for La Pallice micrite; however, differences are observed in their pore size distribution. Most of the pores are concentrated in the pore size range IV = 1–10 μm for Crazannes sparite, and in the range II = 0.01–0.1 μm for La Pallice micrite. As mentioned above, in this article the porosity intervals are defined according to the forces inducing fluid movement through porous media, thus distinguishing between: (i) macroporosity, when the pore size is up to 2500 μm and the fluid mobility is determined by gravitational forces; (ii) mesoporosity, when the pore size is in the 0.1–2500 μm interval and the fluid motion is due to capillary forces; and (iii) microporosity, when the pore size is smaller that 0.1 μm and the fluid motion is caused by adsorption forces. The fluid mobility through porous media due to capillary forces is higher than that due to adsorption forces. According to this, fresh Crazannes sparite is a mesoporous stone (surface area = 1.6 $m^2\ g^{-1}$) and fresh

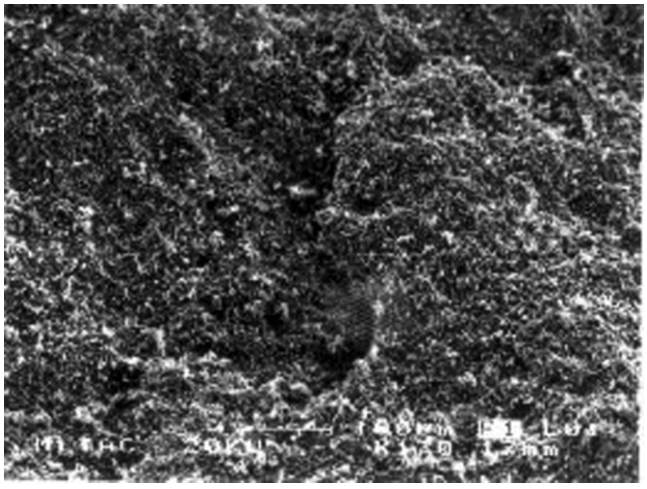

Fig. 5. SEM micrograph of La Pallice micrite. Detail of a single scale in the stone surface.

Table 4
Chemical analysis of soluble salts extracted from Crazannes sparite (CR) and La Pallice micrite (LP) from quarry* and monuments and buildings on the SW coast of France

| # | $Cl^-$ | $NO_3^-$ | $SO_4^{2-}$ | $Mg^{2+}$ | $Ca^{2+}$ | $Na^+$ | $K^+$ |
|---|---|---|---|---|---|---|---|
| CR-1*[a] | 1.5 | n.d. | 0.2 | 0.2 | 7.2 | 1.7 | 0.2 |
| CR-2* | 11 | 0.2 | 2.2 | 1.6 | 9.3 | 14 | 0.3 |
| CR-2P* | 13 | 0.3 | 50 | 1.5 | 65 | 13 | 0.3 |
| CR-3* | 11 | 0.1 | 7.1 | 0.9 | 13 | 14 | 0.1 |
| CR-4*[a] | 3.1 | 0.1 | 0.4 | 0.5 | 9.7 | 2.8 | 0.4 |
| LP-1*[a] | 0.1 | n.d. | 0.1 | 0.3 | 10 | 0.3 | 0.2 |
| LP-2* | 0.1 | n.d. | 0.1 | 0.3 | 7.2 | 0.2 | 0.1 |
| CR-M1 | 27 | 1.6 | 2 | 1.5 | 16 | 14 | 2 |
| CR-M2 | 12 | 5.9 | 6.8 | 0.9 | 28 | 8.5 | 1.7 |
| CR-M3 | 5.4 | 1.7 | 1.1 | 3.5 | 23 | 11 | 1.6 |
| CR-M5 | 16 | 12 | 49 | 1.7 | 74 | 11 | 3.1 |
| CR-M6 | 12 | 16 | — | 3.6 | 229 | 11 | 4 |
| LP-M1 | 8.8 | 9.8 | 5.8 | 3.2 | 28 | 8.6 | 1.2 |
| LP-M5 | 12 | 17 | 1.1 | 2 | 17 | 23 | 1.9 |
| LP-M2 | 3.4 | 2.2 | 0.7 | 1.2 | 9.9 | 2.8 | 0.6 |
| LP-M3 | 5.8 | 23 | 0.5 | 2.7 | 26 | 5.5 | 2.6 |
| LP-M4 | 1.5 | 9.3 | 0.3 | 0.8 | 14 | 1.3 | 0.4 |

Data in meq/100 g; — = not analysed; n.d. = not detected.
[a] Fresh samples.

Table 5
Enrichment factors (EFs) of soluble salts extracted from Crazannes sparite (CR) and La Pallice micrite (LP) from quarry* and monuments and buildings on the SW coast of France vs. seawater

| Samples | $Cl^-$ | $SO_4^{2-}$ | $Mg^{2+}$ | $K^+$ |
|---|---|---|---|---|
| LP-1*[a] | 0.4 | 2.6 | 4.5 | 27 |
| LP-2* | 0.4 | 4.1 | 6.8 | 29 |
| CR-1*[a] | 0.7 | 1 | 0.5 | 4.2 |
| CR-2* | 0.7 | 1.4 | 0.5 | 1.1 |
| CR-2P* | 0.8 | 31 | 0.5 | 1.2 |
| CR-3* | 0.7 | 4.3 | 0.3 | 0.5 |
| CR-4*[a] | 0.9 | 1.3 | 0.7 | 5.8 |
| LP-M1 | 0.9 | 5.6 | 1.6 | 6.2 |
| LP-M5 | 1 | 0.9 | 1.4 | 6.9 |
| LP-M2 | 1.1 | 2.2 | 1.9 | 10 |
| LP-M3 | 0.9 | 0.8 | 2.1 | 21 |
| LP-M4 | 1 | 2.2 | 2.7 | 14 |
| CR-M1 | 1 | 0.7 | 0.5 | 3.8 |
| CR-M2 | 0.7 | 4 | 0.5 | 6.6 |
| CR-M3 | 0.5 | 1.5 | 0.5 | 9 |
| CR-M5 | 1.2 | 36 | 0.7 | 13 |
| CR-M6 | 0.9 | 40 | 1.4 | 17 |

[a] Fresh samples.
* Quarried samples.

La Pallice micrite is a microporous stone (surface area = 5 $m^2\ g^{-1}$).

Weathering of stone implies modification of the porous media, specifically total porosity (TP) and pore size distribution. A variety of patterns is observed in the Crazannes pore network, which suggests that diverse weathering processes should have occurred (visualised already with optical microscopy and SEM). By contrast, in La Pallice micrite, a unique modification pattern is seen in the pore system. Weathering increases total porosity in all samples reaching values up to 25.3%. A net decrease in the number of the smallest pores (I = < 0.01 μm) and an increase in the number of the biggest pores comprised in the microporosity (III = 0.01–1 μm) is detected. In some samples, i.e. LP-1 and LP-M2 but particularly in LP-M5.

### 4.8. Crystallisation pressures

The calculated values of effective pressures for the stones under study are shown in Table 7. Elevated crystallisation pressures were reached. The highest pressures are developed in La Pallice micrite, and in those Crazannes samples with an important percentage of small pores (mainly pores of class II). Most of these crystallisation pressures exceed the tensile strengths of the stones.

## 5. Discussion

### 5.1. Crazannes sparite

There is consensus in the literature that the relative importance of physical and chemical weathering processes for alveoli to develop is related to lithology and structure of rocks, and topographical and environmental conditions [3,4,24,26]. Therefore, alveolar weathering can only be satisfactory explained by invoking the synergism of a range of weathering mechanisms [26].

The results from optical microscopy and SEM show that weathering in Crazannes sparite takes place through

Table 6
Total Porosity (TP) and pore size distribution of Crazannes sparite (CR) and La Pallice micrite (LP) from quarry* and monuments and buildings on the SW coast of France, measured with Mercury Intrusion Porosimetry (MIP)

| # | TP | Φ | s.a. | Pore size distribution | | | | | | | | | |
|---|---|---|---|---|---|---|---|---|---|---|---|---|---|
| | (%) | | | I = < 0.01 μm | | II = 0.01–0.1 μm | | III = 0.1–1 μm | | IV = 1–10 μm | | V = 10–100 μm | |
| | | | | *A* | *B* | *A* | *B* | *A* | *B* | *A* | *B* | *A* | *B* |
| CR-1a*[a] | 14.7 | 2.6 | 1.6 | 0.42 | 2.84 | 1.31 | 8.90 | 2.37 | 16.2 | 9.53 | 64.8 | 1.07 | 7.29 |
| CR-2* | 18.8 | 0.3 | 1.8 | 0.60 | 6.03 | 0.37 | 3.69 | 3.37 | 17.1 | 11.6 | 58.6 | 2.87 | 14.5 |
| LP-1*[a] | 15.2 | 0.9 | 5.0 | 2.00 | 13.1 | 6.46 | 42.3 | 4.65 | 30.5 | 0.75 | 4.91 | 1.39 | 9.14 |
| LP-2* | 18.4 | 0.3 | 3.3 | 0.59 | 3.21 | 4.99 | 27.3 | 10.8 | 59.1 | 1.42 | 7.74 | 0.54 | 2.94 |
| CR-M5 | 16.8 | 0.6 | 1.2 | 0.46 | 2.75 | 0.32 | 1.94 | 2.41 | 14.4 | 11.0 | 65.8 | 2.54 | 15.2 |
| CR-M6 | 10.4 | — | 1.2 | 0.46 | 4.53 | 0.23 | 2.68 | 5.41 | 53.1 | 3.85 | 35.7 | 0.41 | 4.00 |
| CR-M7 | 16.6 | 1.6 | 1.1 | 0.44 | 2.63 | 0.83 | 5.01 | 5.18 | 31.2 | 9.62 | 57.9 | 0.55 | 3.30 |
| CR-M8 | 14.0 | 1.2 | 0.7 | 0.27 | 1.92 | 0.80 | 5.70 | 7.49 | 53.5 | 5.22 | 37.3 | 0.22 | 1.58 |
| LP-M1 | 25.3 | 0.5 | 2.2 | 0.40 | 1.58 | 2.68 | 10.6 | 21.5 | 85.2 | 0.42 | 1.66 | 0.24 | 0.95 |
| LP-M5 | 19.0 | 0.1 | 1.0 | 0.16 | 0.83 | 0.98 | 5.10 | 8.50 | 44.6 | 8.97 | 47.1 | 0.44 | 2.32 |
| LP-M2 | 22.9 | 0.9 | 6.2 | 1.41 | 6.16 | 11.9 | 52.1 | 7.39 | 32.2 | 1.63 | 7.11 | 0.54 | 2.38 |
| LP-M4 | 19.1 | 0.2 | 3.8 | 1.24 | 6.51 | 3.57 | 18.7 | 13.0 | 67.8 | 0.07 | 0.37 | 1.27 | 6.63 |
| LP-M6 | 17.0 | 0.1 | 2.9 | 0.47 | 2.77 | 9.41 | 55.4 | 6.37 | 37.4 | 0.38 | 2.26 | 0.37 | 2.15 |
| LP-M7 | 20.8 | 0.2 | 2.2 | 0.27 | 1.27 | 3.80 | 18.2 | 16.3 | 78.2 | 0.31 | 1.50 | 0.16 | 0.76 |

*A* = porosity (%); *B* = pore volume (%); s.a. = surface area ($m^2\ g^{-1}$); Φ = average pore size (μm); — = not analysed.
[a] Fresh samples.
* Quarried sample

Table 7
NaCl crystallisation pressures developed in Crazannes sparite (CR) and La Pallice micrite (LP) from quarry[a] and monuments and buildings on the SW coast of France

| # | Pore radius range (μm) | | | | | | | | Total pressure (MPa) |
|---|---|---|---|---|---|---|---|---|---|
| | I ($r=0.005$) | | II ($r=0.05$) | | III ($r=0.5$) | | IV ($r=5$) | | |
| | *C* | *P* | *C* | *P* | *C* | *P* | *C* | *P* | |
| CR-1[a,b] | 0.39 | 13.10 | 1.22 | 4.09 | 2.21 | 0.74 | 8.91 | 0.29 | 18.20 |
| CR-2[a] | 0.21 | 6.98 | 0.13 | 0.43 | 1.17 | 0.39 | 4.03 | 0.13 | 7.94 |
| LP-1[a,b] | 1.44 | 48.10 | 4.65 | 15.50 | 3.35 | 1.12 | 0.54 | 0.01 | 64.70 |
| LP-2[a] | 1.09 | 36.50 | 9.24 | 30.90 | 20.0 | 6.69 | 2.63 | 0.08 | 74.10 |
| CR-M5 | 0.18 | 0.60 | 0.13 | 0.42 | 0.95 | 0.31 | 4.34 | 0.14 | 6.93 |
| CR-M6 | 1.12 | 37.50 | 0.56 | 1.87 | 13.2 | 4.41 | 9.39 | 0.31 | 44.10 |
| CR-M7 | 0.80 | 26.70 | 1.51 | 5.04 | 9.42 | 3.15 | 17.5 | 0.58 | 35.50 |
| CR-M8 | 1.23 | 41.00 | 3.64 | 12.10 | 34.0 | 11.40 | 23.7 | 0.79 | 65.30 |
| CR-M9 | 3.68 | 123.0 | 18.7 | 62.50 | 42.8 | 14.30 | 2.14 | 0.07 | 200 |
| LP-M1 | 1.67 | 55.70 | 11.2 | 37.30 | 89.7 | 30.00 | 1.75 | 0.05 | 123 |
| LP-M5 | 0.36 | 12.10 | 2.23 | 7.44 | 19.3 | 6.45 | 20.4 | 0.68 | 26.70 |
| LP-M2 | 2.61 | 87.20 | 22.1 | 73.90 | 13.7 | 4.57 | 3.02 | 0.10 | 166 |
| LP-M4 | 0.98 | 32.60 | 2.81 | 9.39 | 10.2 | 3.41 | 0.06 | 0 | 45.40 |
| LP-M6 | 1.27 | 42.40 | 25.4 | 84.90 | 17.2 | 5.75 | 1.03 | 0.03 | 133 |
| LP-M7 | 1.69 | 56.40 | 23.7 | 79.30 | 102 | 34.00 | 1.94 | 0.06 | 170 |

$r$ = Radius of pore classes (μm); $C = V_r/V_R$; $P$ = crystallisation pressure (MPa). Theoretical crystallisation pressures (MPa): I = 334; II = 33.4; III = 3.34; IV = 0.33. $V_r$ = volume percent of small pores of each class of pores (I to IV). $V_R$ = volume percent of large pores of each class of pores (I–IV).

[a] Samples from quarry.

[b] Fresh samples.

the following combined chemical and physical processes which lead to granular disaggregation and ultimately to alveolar weathering: cement dissolution, chemical decomposition and physical action of salt crystallisation. Comparing the petrographic characteristics of fresh and decayed stones, it is concluded that cement dissolution is due to the action of sea-salt spray, since no dissolution was observed in fresh, sheltered stones in quarry. The ionic strength of the saline solution that wets the stones under direct exposure to salt spray effect should increase the dissolution of the cement [27]. However, the medium-grained texture and the homogeneous network of Crazannes sparite also have favoured the dissolution. The carbonate cement dissolution leads to a well-connected porous network, and as a consequence, favours an increment of the total porosity. This allows a deeper capillary migration of solutions towards the interior of the stone. Therefore, the quantity of solution that accesses and moves inward in Crazannes sparite is higher than in the fresh stones (and also higher than in the dense La Pallice micrite, as will be discussed). Higher total porosity allows a more intense evaporation, which in turn enhances the inward movement of soluble salts by capillary action. The intense evaporation that has operated in the Crazanne stone is put in evidence by the non-equilibrium, anhedral crystal forms in its pores observed with SEM. These morphologies crystallise under high supersaturation ratios [28,29] which, it is suggested, are reached through intense evaporation processes, since high supersaturation ratios achieved by cooling and/or changes in the chemical potential of solution are considered negligible in the current study.

The SEM observations show also that salts are found deeper in Crazannes sparite than in the more dense and homogeneous La Pallice micrite, in agreement with the findings of Cardell et al. [13] who determined and quantified the porosity and salts with depth for these calcareous stones. Low silicate dissolution rates followed by precipitation of silica amorphous layers were also observed with SEM. Quartz is far more soluble in near-surface environments than was originally thought. Chemically weathered quartz grains have been described [30], and it is established that silica dissolution is enhanced under saline conditions (e.g. by sodium chloride [3]. Considering the above mentioned, it is suggested that the etching features observed in some quartz grains can be due to the effect of salt loading from sea spray.

The results of EFs for most of the salts in Crazannes stones indicate the marine origins of the measured ions, with some exceptions, as for instance, the anthropogenic origin for $SO_4^{2-}$ identified in black crusts. The high EF for $K^+$ in samples from the church of St. Sauvier in La Rochelle can be explained by local enrichment due to bird droppings, since pigeon nests are spread all over the walls and roof.

Weathering of stone implies modification of the porous media, specifically in total porosity and pore size distribution. Interpretation of the changes observed in the pore system of Crazannes sparite (determined with

MIP) is complicated, since these changes are the response to the synergistic action of salt crystallisation, cement dissolution and overgrowth and/or recrystallisation. The correct interpretation should be supported by macro- and microscale observations of the decay forms operating in this stone type. Total porosity (TP) increases in those samples showing granular disintegration, by contrast TP diminishes in those samples showing efflorescences, since these occlude the pores. The increase in TP and in the number of mesopores in samples CR-2 and CR-M5 may be the result of cement dissolution and physical action of salt crystallisation pressure. The microporosity genesis in samples CR-M7 and CR-M8 can be explained by occlusion of mesopores due to crystallised salt. The decrease in TP in sample CR-M6, which is a black crust, is considered to be the result of the entrapment of minerals, salts and particles (observed by SEM-EDX).

Determining the stone susceptibility to salt crystallisation pressure using structural and mechanical parameters is well reported in literature [8,9,20,22,31]. Breakage of stone is due to physical action of salts crystallising into its pore network when crystallisation pressure exceeds the tensile strength of the stone. Very high crystallisation pressures were obtained for weathered Crazannes stones, ranging from 35.5 to 200 MPa, which far exceed the tensile strength of 0.9 MPa calculated by Auger for fresh Crazannes stones [1]. This suggests that, besides the above mentioned weathering mechanisms, crystallisation pressure appears to be the main mechanism generating weathering in Crazannes stone, since other salt damage mechanisms, as for instance hydration pressure, thermal expansion and chemical weathering, are assumed to have little relevance to the current deterioration observed in the stone types under study, for which crystallisation due to evaporation appears to be the most important process.

### 5.2. La Pallice micrite

The high concentrations of Si, K, Ti, Mn, Ni, Rb and Sr detected with EDX-RF in La Pallice micrite are considered to be due to the presence of phyllosilicates and Fe-oxi-hydroxides that make up this stone type. The results of enrichment factors (EFs) show high values for $K^+$ in all La Pallice samples which suggest that bird droppings are the most probable sources for samples taken in La Rochelle, and biological activity for the rest of the samples, since abundant plants were observed on the sampled buildings. The high EFs for $Mg^{2+}$ may be due to the phyllosilicates that make up this stone.

The optical microscopy observations suggest that the isolated micro-fissures appearing near the stone surface should be the first step in the weathering of La Pallice micrite, where flaking is the macro-scale weathering form. When weathering progresses and fissures coalescence, an interconnected fissure network is formed penetrating deeper inside the stone. Detachment of the stone material ultimately occurs and multiple fissures are the macro-scale weathering form observed in field. Chemical weathering was not observed, which is likely due to the low reactivity of the micrite calcite crystals that made the cement.

The optical and electronic microscopy reveal that salts crystallise at or near the surface, because the dense crystalline texture does not facilitate water and vapour transfer inside the stone. This also explains the low evaporation rates that operate in La Pallice micrite, which are put in evidence by the euhedral and/or whisker-like crystals observed with SEM. These crystalline morphologies suggest that they were formed at low supersaturation ratios [28,29], which only can be achieved with low degree of evaporation. Indeed, our field observations corroborate that La Pallice stone remains wet over a period of several days after a rainfall.

The results from MIP suggest that the changes induced in the pore system of La Pallice stone are due to the disruptive effect of salt crystallisation, since the total porosity has increased in all the samples. Thus, mesoporosity is generated as result of micro-fissure coalescence leading to larger and multiple fissures (as observed with optical microscopy).

Regarding the crystallisation pressures obtained for La Pallice micrite, they largely exceed the value of tensile strength for this stone obtained by Auger [1]. However, for those samples with crystallisation pressure values (e.g. LPM-4 and LPM-5) that do not surpass the value of tensile strength, we can argue that disruption of the stone can be achieved because crystallisation from saline solutions favours propagation of fissures reducing the mechanical strength of this stone [32], thus La Pallice stone can suffer severe damage even when salts exert little pressure.

### 5.3. The weathering mechanisms due to salt spray

Although some deterioration appears in stones near ground level, most of the weathered stones are observed on the median-high parts of monuments and buildings, where the supply of ground water to stone is limited. Therefore, for these stones that receive water in a gaseous phase, salt crystallisation mechanism should be associated with sea-spray deposition, and the weathering process cannot be explained considering the same process involved in salt crystallisation when water is supply by capillary penetration from ground. Weathering should be discussed through wet/dry or moist/dry cycles. As Cardell et al. demonstrated [27], salt weathering that takes place in coastal areas is best reproduced in laboratory using a salt-weathering test in which stones are weathered in a controlled chamber that reproduces cycles of saline spray and drying.

With this in mind, for salt crystallisation weathering to proceed, salts must be dissolved such that the original solution penetrates towards the inside of the stone where it will evaporate. To form a solution, it is necessary to have a water source other than rainwater, which leaches salts from the stone surface. Water vapour proceeds from sea-spray droplets, whose input has been confirmed by the enrichment factors (EFs). Condensation phenomenon can also wet stone surfaces [33]. Then, a brine solution has to be formed and, before drying, has to wet the stone surface long enough to migrate towards inside the stone. Saline spray transport mainly occurs via laminar viscous flow according to Darcy's law thus, the vapour flux of a saline solution (and therefore the amount of salts entering the stone) is governed by the specific permeability, which in turn is governed by the porosity and pore radii of stone. Therefore, in stones with a pore system built up of small pores (e.g. La Pallice micrite), water vapour transport will be slow and will migrate inside the stone to a lesser extent. By contrast, in stones with a pore system made up of meso- and macropores (e.g. Crazannes sparite), the greater porosity allows the access of more solution and further migration inside the stone. As well, it should be considered that high total porosities enhance saline solution uptake. The problem of moisture in buildings has always generated great interest. The mechanisms that control the transport of moisture in a wall are complex, we can refer to the works of De Freitas et al. [33], Camuffo [34] and Mosquera et al. [35].

High relative humidities like the ones reported in the current area (e.g. average yearly RH = 79%, max. RH = 100% and min. RH = 73%), and variation of the relative humidity through 75% (the equilibrium relative humidity for NaCl at 25 °C is 75.03%) may allow solution formation. Thus, for relative humidities $>75\%$, water fixation led to dissolution of salts present in the stones. The solution penetration is determined by the pore network. Obviously, in the current study, the moisture front is different for both Crazannes and La Pallice stones, and therefore, the position of salts (when evaporation of saline solution induces crystallisation) in relation to the stone surface is also different. As discussed by Snethlage and Wendler [36], the maximum of moisture content resulting from wet/dry cycling is closer to the surface in denser stones, as La Pallice micrite is, and deeper and broader in coarse porous media, as in the case of Crazanne sparite. It is the position of salts which determines largely the weathering forms developed in these stones.

The literature reports that stones with high proportions of micropores are more susceptible to salt decay than those with high proportions of large pores [9,22]. However, the results obtained in this study show that anomalies limit the extent to which this generalisation can be made, since Crazannes sparite is eventually weathered more severely than La Pallice micrite. This observation is consistent with the findings of Cardell et al. [27] who observed, after submitting stones with different pore systems to a salt-spray crystallisation test, that greater porosity (allowing more solution to enter the stone) led to more intense weathering. Other authors state that the importance of pore size lies in its effect on the extent and rate of evaporation of salt solutions [37,38].

The well-connected network of Crazannes sparite, built up of mesopores, should allow capillary transfer over large distances inside the stone (capillary coefficient of approx. 17.1 kg $m^{-2}$ $s^{0.5}$), but also good evaporation, which occurs not at the very surface but deeper within the stone. When a salt solution reaches supersaturation, salt crystallises and physical disruption of the sparite occurs because the developed crystallisation pressures exceed its tensile strength. Cement dissolution should act synergistically. Roughness and irregularities in the Crazannes stone surface also favour alveolar weathering, since areas with higher porosity and surface area are potentially more favourable to absorb salt solutions. The literature states that alveolar weathering is a result of the stone's heterogeneity [22,39]. The rough surface of Crazannes sparite also enhances uptake of pollutant elements such as Pb (detected with EDX-FR).

However, wind action is invoked for alveoli to develop in Crazannes stone. Our field observations reveal that, in the sheltered Crazannes quarry, no alveolar weathering is observed in stones. By contrast, Crazannes sparite develops spectacular alveoli once placed in monuments and buildings exposed to overall winds, and storms. Wind action is reported in the literature as a key factor for the formation of alveolar weathering [40,41]. Moreover, wind action is essential for removing debris from the interior of the cavities, which in the current area can be done by marine breezes, such that alveolar weathering is known to be a self-propagating process [42].

In La Pallice micrite, its interlocking texture and pore system built up of small isolated pores prevent the initial uptake of salt solutions from sea-spray. However, surface irregularities such as original fissures or other weak points (e.g. clay minerals observed with microscopic techniques) facilitate penetration of salt solutions. The limited capillary transfer (capillary coefficient = 1.40 kg $m^{-2}$ $s^{0.5}$) and slow water vapour transport deter transfer of solution inside the stone. Therefore, evaporation and subsequent salt crystallisation will take place at or just below the stone surface. While the literature reports that salts crystallising at or near stone surface only cause aesthetic problems [2,24], our results shows that salts crystallising near the La Pallice micrite surface generate crystallisation pressures high enough to exceed its tensile strength (approx. 6.1 MPa), leading to the formation of fissures and eventually scales which ultimately disrupt

the stone. However, as we discuss next, other deterioration mechanisms are suggested to be involved in the weathering that leads to La Pallice stone breakage.

Our field observations confirm that freshly quarried La Pallice micrite can disrupt through flaking and fissuring patterns over the course of 15 years, once it placed in buildings and monuments. Because of this, complete stone replacements are often required during renovation work in the city of La Rochelle. We think that a different deterioration mechanism other than salt crystallisation has to act synergistically for weathering to proceed in La Pallice micrite in this timespan. Observations of rock flaking are thought to reflect the impact of thermal stress [43].

The fact that flakes observed under SEM run parallel to the stone surface suggest that delimiting microfractures are related to environmental cycles of heating/cooling and/or wetting/drying. Salt weathering experiments have shown that scales (i.e. flakes) form when salts crystallise in a sub-surface zone related to a frequent wetting depth with dilute salt solutions [44]. Crack propagation can also be enhanced by the presence of saline solution while crystals precipitate as discussed by Dunning and Huf [45].

Short-term fluctuation of temperatures in La Pallice stone surface can be achieved in the current area in response to variations in wind-speed and cloud cover, and may ultimately contribute to stone breakdown through 'fatigue' effects. Although the stresses generated in this way are small compared to the tensile strength of La Pallice micrite, high frequency stress events may gradually reduce the cohesive strength of intergranular bonds and initiate microfracture development. With this in mind, we can argue that 'fatigue' effects may also contribute to stone breakdown by facilitating the ingress and enhancing the effectiveness of weathering agents such as salt and moisture. Scale development appears to be inhibited on the heterogeneous sandstone as it was observed by Smith et al. in Belfast buildings stone [46].

## 6. Conclusions

This article has focused on the weathering forms identified in monuments, buildings and quarries on the SW coast of France, and made inferences concerning the deterioration processes responsible for their development. The stone types under study decay due to salt weathering as a consequence of their location in marine environment. Laboratory analysis and micro-morphological studies indicate that diverse deterioration processes operate synergistically on each stone types leading to different weathering patterns: sanding and alveolar weathering in the heterogeneous Crazannes sparite; and fissuring and flaking in the homogeneous La Pallice micrite.

Physical stress resulting from salt crystallisation in pores is the most important deterioration mechanism causing breakage of both stone types. In Crazannes sparite, alveolar weathering takes place through mechanical action of salt crystallisation and granular disintegration, the latter as a result of carbonate cement dissolution. Its heterogeneous texture plus wind turbulence created by e.g. marine breezes favour its uneven breaking. By contrast, La Pallice micrite with a homogeneous and interlocking crystalline texture develops a flaking pattern due also to salt crystallisation, but 'fatigue effects' due to thermal stress also should be consider. Weathering starts by forming isolated microfissures sub-parallel to the surface. A multiple fissure network is formed when fissures expand and penetrate deeper into the stone. The structure of these stones controlling their actual distribution of moisture and water content is the key factor for different weathering patterns to develop, other factors being similar, as for example, the rock mineralogy and environmental conditions.

The results obtained in this work show that anomalies limit the extent to which generalisations can be made. In both stone types salt weathering leads finally to stone breakage. This shows that under suitable conditions both coarsely porous stone and finely porous stone can be highly susceptible to salt decay.

A conservation policy for the building materials studied here, exposed to marine environment (and not in direct contact with water-splash), only can be established by improving routine maintenance practices. This involves developing the most suitable salt extraction procedures followed by the right consolidation and protection interventions according to the stone types. In any case chemical, physical and mechanical studies of the stones are required. In particular, the pore systems should be characterised since they control their process rates and forms of deterioration.

## Acknowledgments

The European Community under contract ENV4-CT95-0100 financed this study. We are indebted to T. Rivas (Univ. of Santiago de Compostela, Spain) for her indispensable help in the realisation of this work. We also thank M.J. Mosquera (Univ. of Cadiz, Spain) for the porosimetric measurements and A. Kowalski for helping with the manuscript.

## References

[1] Auger F. Alteration des roches sous influence marine; degradation des pierres en oeuvre et simulation acceleree en laboratoir. These Doctorat d'Etat es Siences. Universite de Poitiers, France (1987).

[2] Lewin SZ. The mechanism of masonry decay through crystallisation. In: Barkin SM, editor. Conservation of Historic Stone Buildings and Monuments. Washington DC: National Academy of Sciences, 1981. p. 120–44.

[3] Young ARM. Salt as an agent in the development of cavernous weathering. Geology 1987;15:962–6.
[4] Pye K, Mottershead DN. Honeycomb weathering of carboniferous sandstone in a sea wall at Weston-super-Mare, UK. Q J Eng Geol 1995;28:333–47.
[5] Zezza F. Marine spray and polluted atmosphere as factors of damage to monuments in the Mediterranean coastal environment. In: Zezza F. Ed. Bari. Origin, mechanisms and effects of salts on degradation of monuments in marine and continental environments. Protection and conservation of the European Cultural Heritage, E.C. Project, Report 4. (1996) p. 3–19.
[6] Zezza F, Macri F. Marine aerosol and stone decay. Sci Total Environ 1995;167:123–43.
[7] Moropoulou A, Theoulakis P, Chrysophakis T. Correlation between stone weathering and environmental factors in marine atmosphere. Atmos Environ 1995;29(8):895–903.
[8] La Iglesia A, Garcia del Cura MA, Ordonez S. The physicochemical weathering of monumental dolostones, granites and limestones; dimension stones of the Cathedral of Toledo (Spain). Sci Total Environ 1994;152:179–88.
[9] Theoulakis P, Moropoulou A. Microstructural and mechanical parameters determining the susceptibility of porous building stones to salt decay. Constr Build Materials 1997;11(1):65–71.
[10] Fitner B, Heinrichs K, Kownatzki R. Weathering forms—classification and mapping. Verwitterungsformen-Klassifizierung und kartierung.-Denkmalpflege und Naturwissenschaft, Natursteinkonservierung I: forderprojekt des bundesministeriums fur Bildung, Wissenschaft, Forchung und Technologie. Berlin: Verlag Ernst and Sohn, 1995.
[11] Raccomandazioni NORMAL–1/88. Alterazioni macroscopiche dei materiali lapidei: lessico. CNR–ICR Roma 1990.
[12] Folk RL. Am Assoc Petrol Geol Bull 1959;43:1–38.
[13] Cardell-Fernández C, Yebra A, Van Grieken R. Combined digital image processing-SEM-EDX and BSE data acquisition to determine porosity and salt distribution in-depth in porous materials: a methodology to quantify salt weathering. Mikrochemica Acta 2002;140:9–14.
[14] Schneider B. Source characterisation for atmospheric trace metals over Kiel Bight. Atmos Environ 1987;21:1275–83.
[15] Riley JP, Chester R. Introduction to Marine Chemistry. London: Academic Press, 1971.
[16] Torfs K, Van Grieken R. Chemical relations between atmospheric aerosols, deposition and stone decay layers on historic buildings at the Mediterranean coast. Atmos Environ 1997;31:2179–92.
[17] Evans IS. Salt crystallisation and rock weathering: a review. Revue de Géomorphologie Dynamique 1970;19:155–77.
[18] Everett DM. The thermodynamics of frost damage to porous solids. Trans Faraday Soc 1961;57:2205–11.
[19] Wellman HW, Wilson AT. Salt weathering, a neglected geological erosive agent in coastal and arid environments. Nature 1965;205:1097–8.
[20] Fitzner B, Snethlage R. Uber zusammenhange zwischen salzkristallisationsdruck und porenradienverteilung. GP News Letter 1982;3:13–24.
[21] Welman HW, Wilson AT. Salt weathering or fretting. In: Fairbridge RW, editor. The Encyclopedia of Geomorphology.Stroudsburg, Pennsylvania, 1968. p. 968–70.
[22] Rossi-Manaresi R, Tucci A. Pore structure and the disruptive or cementing effect of salt crystallisation in various types of stone. Stud Conserv 1991;36:53–8.
[23] Benavente D, García del Cura MA, Fort R, Ordóñez S. Thermodynamic modelling of changes induced by salt pressure crystallisation in porous media of stone. J Cryst Growth 1999;204:168–78.
[24] Rodriguez-Navarro C, Dohene E. Salt weathering: influence of evaporite rate, supersaturation and crystallisation pattern. Earth Surf Processes Landforms 1999;23(3):191–209.
[25] Griffith AA. Theory of rupture. Proc. 1st Int. Congr. Appl. Mech. Delft. 1924. p. 55–63.
[26] Turkington AV. Cavernous weathering in sandstone: lessons to be learned from natural exposure. Q J Eng Geol 1998;31:375–83.
[27] Cardell C, Rivas T, Mosquera MJ, Birginie JM, Moropoulou A, Prieto B, Silva B, Van Grieken R. Patterns of damage in igneous and sedimentary rocks under conditions simulating sea-salt weathering. Earth Surf Processes Landform, in press, 2002.
[28] Sunagawa I. Characteristics of crystal growth in nature as seen from the morphology of crystals. Bull Min 1982;104:81–7.
[29] Zenhder K, Arnold A. Crystal growth in salt efflorescences. J Cryst Growth 1989;97:513–21.
[30] Pye K, Sperling B. Experimental investigation of silt formation by static breakage processes: the effect of temperature, moisture and salt on quartz dune sand and granitic regolith. Sedimentology 1983;30:49–62.
[31] Benavente D, García del Cura MA, Bernabéu A, Ordóñez S. Quantification of salt weathering in porous stones using an experimental continuous partial immersion method. Eng Geol 2001;59(3–4):313–25.
[32] Dunnig JD, Huf WL. The effects of aqueous chemical environments and hydraulic fracture propagation and morphologies. J Geophys Res 1983;88:6491–9.
[33] De Freitas VP, Abrantes V, Crausse P. Moisture migration in building walls. Analysis of the interface phenomena. Build Environ 1996;31(2):99–108.
[34] Camuffo D. Condensation–evaporation cycles in pore and capillary systems according to the Kelving model. Water Air Soil Pollut 1984;21:151–9.
[35] Mosquera MJ, Rivas T, Prieto B, Silva B. Capillary rise in granitic rocks: interpretation of kinetics on the basis of pore structure. J Colloid Interface Sci 2000;222:41–5.
[36] Snethlage R, Wendler E. Moisture cycles and sandstone degradation. In: Baer NS, Snethlage R, editors. Saving our Architectural Heritage. The Conservation of Historic Stone Structures. Chichester: Elsevier, 1997.
[37] Leith SD, Reddy MM, Ramirez WF, Heymans MJ. Limestone characterisation to model damage from acidic precipitation: effect of pore structure on mass transfer. Environ Sci Technol 1996;30:2202–10.
[38] McGreevy JP. Pore properties of limestone as controls on salt weathering susceptibility: a case study. Processes Urban Stone Decay 1996;13:50–167.
[39] Chabas A, Jeannette D. Weathering of marbles and granites in marine environment: petrophysical properties and special role of atmospheric salts. Environ Geol 2001;40(3):359–68.
[40] Rodriguez-Navarro C, Dohene E, Sebastian-Pardo E. Origin of honeycomb weathering: the role of salts and wind. Geol Soc Am Bull 1999;111:1250–5.
[41] Rossi-Manaresi R. Pietre porose: alterazione conservazione in materiali lapidei. Bolletino d'Arte 1987;41:133–44.
[42] Dorn RI. Digital processing of backscatter electron imagery: a microscopic approach to quantifying chemical weathering. Geol Soc Am Bull 1995;107:725–41.
[43] Hall K, André MF. New insights into rock weathering form high-frequency rock temperature data: an Antartic study of weathering by thermal stress. Geomorphology 2001;41(1):23–35.

[44] Smith BJ, McGreevy JP. Contour scaling of a sandstone by salt weathering under simulated hot desert conditions. Earth Surf Processes Landforms 1988;13:697–706.
[45] Dunning JD, Huf WL. The effects of aqueous chemical environments on crack and hydraulic fracture propagation and morphologies. J Geophys Res 1983;88:6491–9.
[46] Smith BJ, Magee RW, Whalley WB. Breakdown patterns of quartz sandstone in a polluted urban environment, Belfast, Northern Ireland. In: Robinson DA, Williams BG, editors. Rock Weathering and Landform Evolution. John Wiley & Sons Ltd, 1994.